(Received 8 January 2026, Accepted 30 January 2026, Scheduled 19 February 2026)

Non-Contact Vital Sensing Using Millimeter-Wave MIMO FM-CW Radar Based on Two-Wave Model and Considering Slight Body Movement

Mie Mie Ko and Toshifumi Moriyama*

Graduate School of Engineering, Nagasaki University, 1-14, Bunkyo-machi, Nagasaki 852-8521, Japan

ABSTRACT: Radar-based vital sensing methods have received significant attention due to their potential to provide continuous, non-contact measurements for heartbeat and respiration monitoring. Our original two-wave model extracts respiration and heartbeat data by formulating the estimation process as a minimization problem. Although the original method examines temporal changes in respiration and heartbeat signals in a different manner from existing methods, it remains sensitive to the slight body movements that often occur in laboratory experiments. In this study, we propose a modified two-wave model with improved robustness against such movements. Using experimental data collected with a millimeter-wave Multi-Input Multi-Output (MIMO) frequency-modulated continuous-wave (FM-CW) radar system, we demonstrate that the improved model can successfully measure both respiration and heartbeat signals even in cases where the original method fails, thereby improving the capability for non-contact vital signal detection.

1. INTRODUCTION

The research on heartbeat and respiration monitoring using radar has recently gained significant attention [1–11]. Although wearable sensors are useful for measuring these vital signals, they may cause skin irritation, and their batteries require frequent recharging, making them less convenient for continuous use. Therefore, non-contact vital sensing using radar has emerged as a promising alternative, enabling continuous monitoring without the discomfort or maintenance issues associated with wearable devices. Three types of radars are used for vital sensing: continuous-wave (CW) [1, 2, 10], frequency-modulated continuous-wave (FM-CW) [3, 4, 7, 11], and ultra-wideband (UWB) [5, 6]. Radar systems typically measure heartbeat and respiration rates according to their periodicity, which is obtained through arctangent demodulation of complex (IQ) radar signals [2–4]. However, even slight body movements (such as those occurring when measurements are taken while sleeping or sitting in a chair) can disrupt these periodic patterns, making their accurate measurement challenging. Therefore, motion compensation and signal separation techniques, which are particularly complicated forms of processing are essential for improving the robustness of vital sign detection methods [10, 11]. We previously proposed a two-wave model based on Fourier series expansion to extract respiration and heartbeat data by formulating the estimation process as a minimization problem [7]. The use of a window function in the minimization problem allows us to evaluate temporal changes such as the respiration rate, heartbeat rate, and interbeat interval (IBI) of the heartbeat. In [7], when performing measurements while the target was sleeping, the measurement accuracy of the IBI was 97.09% compared with that obtained with a contact sensor. Although this approach is also affected by body movements, improvements to the model can enhance its robustness, enabling accurate and simultaneous measurement of heartbeat and respiration data even in the presence of motion.

In this study, we present a modification of our two-wave model and, using experimental data obtained from a millimeter-wave Multi-Input Multi-Output (MIMO) frequency-modulated continuous-wave (FM-CW) radar system operating in the 77–80 GHz frequency band, demonstrate that it can accurately measure respiration and heartbeat waveforms even in cases where the original model fails. The remainder of this paper is organized as follows. Section 2 provides the process of phase measurement with MIMO FM-CW radar to detect vital signals. Section 3 describes the modification of our two-wave model and parameter estimation method to account for body movement. Section 4 presents our experimental results and discusses associated issues. Finally, the conclusions are presented in Section 5.

2. PHASE MEASUREMENT OF MIMO FM-CW RADAR

In this study, a MIMO FM-CW radar system was used for vital sensing. The FM-CW radar outputs a discrete complex beat signal $S_b(mn)$ after quadrature detection and A/D conversion

$$S_b(m,n) = Ae^{jk_0R_m}e^{j2\pi M\frac{R_m}{c}nt_s} \quad (1)$$

$$R_m = 2R_0 + md\sin\theta_0 \quad (2)$$

where A is the beat signal amplitude; $k = 2\pi/\lambda_0$ is the wave number of the center frequency of the FM-CW signal, where λ_0 is the wavelength. $M = B/T$ is the frequency modulation

* Corresponding author: Toshifumi Moriyama (t-moriya@nagasaki-u.ac.jp).

slope, where B and T are the bandwidth and time width of the FM-CW signal, respectively; c is the speed of light; t_s is the A/D converter sampling time; n is the time index; d and m are the antenna spacing and antenna element index, respectively; and R_m is the round-trip distance between the m-th antenna and the target. It is assumed that the azimuth angle relative to the antenna array of the monitored target is θ_0 and that the antenna array is one-dimensional, as defined in [7]. After Discrete Fourier Transform (DFT) processing, the beat spectrum is:

$$\begin{aligned} S_b'(m,k) &= \sum_{n=0}^{N-1} S_b(m,n)\, e^{-j\frac{2\pi n}{N}k} \\ &= Ae^{jk_0R_m} \frac{\sin\left[\pi N\left(M\frac{R_m}{c}t_s - \frac{k}{N}\right)\right]}{\sin\left[\pi\left(M\frac{R_m}{c}t_s - \frac{k}{N}\right)\right]} \\ &\quad e^{j\pi(N-1)\left(M\frac{R_m}{c}t_s - \frac{k}{N}\right)}. \end{aligned} \tag{3}$$

At the target position ($MR_mt_s/c - k/N = 0$), Eq. (3) can be approximated as

$$S_b'(m) \approx ANe^{jk_0R_m}. \tag{4}$$

In addition, when the beamforming process is applied to Eq. (4),

$$\begin{aligned} S_b''(\theta) &= \sum_{m=0}^{M-1} S_b'(m)\, e^{-jk_0md\sin\theta} \\ &= ANe^{jk_02R_0} \frac{\sin\left[\frac{k_0dM}{2}(\sin\theta_0 - \sin\theta)\right]}{\sin\left[\frac{k_0d}{2}(\sin\theta_0 - \sin\theta)\right]} \\ &\quad e^{jk_0d\frac{M-1}{2}(\sin\theta_0 - \sin\theta)}. \end{aligned} \tag{5}$$

Under the target direction ($\sin\theta_0 - \sin\theta = 0$), Eq. (5) can be approximated as

$$S_b''(m) \approx ANMe^{jk_02R_0}. \tag{6}$$

This process generates a two-dimensional image in the slant range and azimuth directions, which can provide information on the target position. In Eq. (6), the exponential term includes the distance (R_0) between the radar and the target, where the phase is expressed as

$$\theta = 2k_0R_0 \tag{7}$$

The radar measures the target repeatedly, where the time interval between the transmitting waves is called pulse reparation interval (PRI). This allows the radar to detect small displacements of the target at each PRI. However, the phase provides a value within the interval $(-\pi, \pi]$ or $[0, 2\pi)$, or the wrapped phase [8]. Therefore, phase unwrapping must be applied to the measured data.

3. PARAMETER ESTIMATION METHOD FOR BODY MOVEMENT

Although some studies have evaluated time-averaged respiration and heartbeat rates using the Fourier transform, the purpose of this study is to enable the estimation of individual respiration and heartbeat. Their waveforms are similar to periodic functions, such as square or triangular waves, which are expressed as a combination of harmonics in Fourier series expansions. However, the period of the phase waveform associated with the heartbeat or breathing is not constant throughout the entire observation duration. Therefore, it is assumed that the waveform within one or two periods can be represented as a Fourier series expansion. In this section, we provide a brief explanation of our previous two-wave vital radar sensing model based on Fourier series expansions, followed by the proposed method, and alter it to account for slight body movements.

3.1. Two-Wave Model

The original model assumes that a person is stationary and that the skin on their chest vibrates due to respiration and heartbeat. The phase of the radar echo from the chest skin (given by Eq. (7)) is affected by these vibrations. Thus, the phase $\theta^{two}(t)$ is modeled as

$$\theta^{two}(t) = \theta_r(t) + \theta_h(t). \tag{8}$$

where $\theta_r(t)$ and $\theta_h(t)$ are the phase terms of the respiration and heartbeat signals of the target, respectively, as functions of the time t. Although noise affects the phase, it is omitted in Eq. (8). In particular, $\theta_r(t)$ and $\theta_h(t)$ are represented as finite sums of the sine and cosine harmonics at frequencies f_r and f_h whose center time is t_0 based on the trigonometric Fourier series as follows:

$$\begin{aligned} \theta_r(\mathbf{p}_r(t_0), t) = a_{0,r} + \sum_{q=1}^{Q} \{a_{q,r}\cos[2\pi q\, f_r(t-t_0)] \\ + b_{q,r}\sin[2\pi q f_r(t-t_0)]\} \end{aligned} \tag{9}$$

$$\begin{aligned} \theta_h(\mathbf{p}_h(t_0), t) = a_{0,h} + \sum_{p=1}^{P} \{a_{p,h}\cos[2\pi p\, f_h(t-t_0)] \\ + b_{p,h}\sin[2\pi p f_h(t-t_0)]\} \end{aligned} \tag{10}$$

where $\mathbf{p}_r(t) = [a_{0,r}, a_{1,r}, \ldots, a_{Q,r}, b_{1,r}, \ldots, b_{Q,r}, f_r]$ and $\mathbf{p}_h(t) = [a_{0,h}, a_{1,h}, \ldots, a_{P,h}, b_{1,h}, \ldots, b_{P,h}, f_h]$ are the weighting parameters and fundamental frequencies of the respiration and heartbeat phases, respectively [7]. These harmonics contribute to the representation of asymmetric waveforms. Furthermore, Q and P are the maximum-orders of harmonics, which depend on the signal-to-noise ratio (SNR) and measurement conditions for the estimation of $\mathbf{p}_r(t_0)$ and $\mathbf{p}_h(t_0)$. According to previous studies, the maximum orders can be evaluated as Q up to 2 or 3 and P up to 1. Unfortunately, as $P = 1$ represents a symmetric sinusoidal waveform, a detailed estimation of the heartbeat waveform is difficult. In rare cases, the triple frequency ($3f_r$) of respiration may coincide with the fundamental frequency (f_h) of the heartbeat. In this situation, analysis should be performed with $Q = 2$ [7].

3.2. Modified Two-Wave Model for Slight Body Movement

In Eqs. (9) and (10), $a_{0,h}$ and $a_{0,r}$ are constant numbers that express the DC component, meaning that this model does not

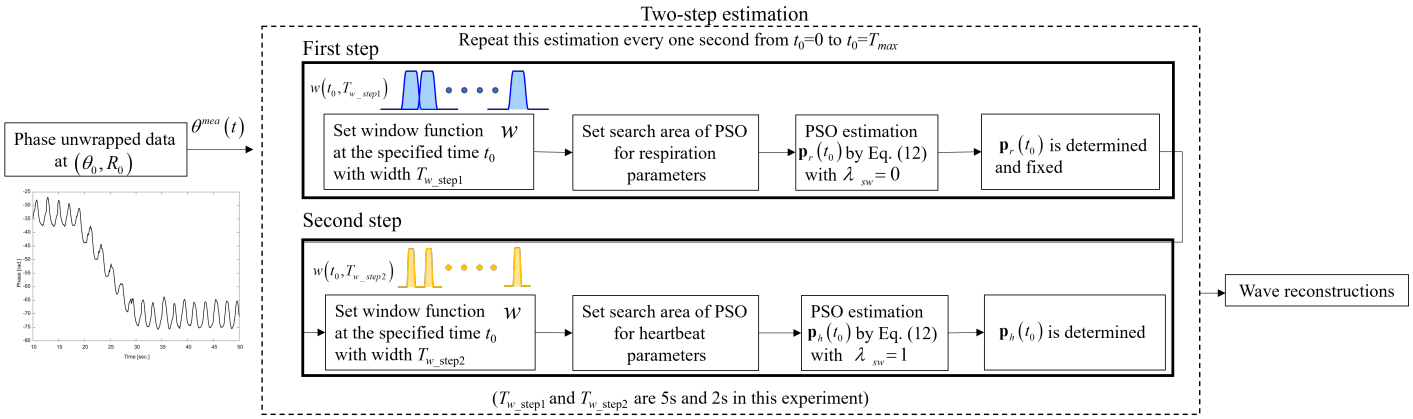

FIGURE 1. Flowchart of two-step estimation process.

consider body movements. Therefore, higher-order harmonics are needed if the target moves, and parameter estimation becomes complicated due to the many unknowns. To overcome this problem, Eq. (9) is modified by adding a term for the consideration of slight target motions $a_{Q+1,r}(t-t_0)$, which indicates the linear motion of the target.

$$\theta_r'(\mathbf{p}_r(t_0),t) = a_{0,r} + a_{Q+1,r}\,(t-t_0) + \sum_{q=1}^{Q}\{a_{q,r}\cos\left[2\pi q\, f_r\,(t-t_0)\right] + b_{q,r}\sin\left[2\pi q\, f_r\,(t-t_0)\right]\} \quad (11)$$

The first two terms above represent body movements, while the remaining terms represent respiration.

3.3. Unknown Parameter Estimation

To estimate the unknown parameters in Eqs. (10) and (11) at a specified time t_0, the following cost function is used:

$$\Phi(t_0,\mathbf{p}_h(t_0),\mathbf{p}_r(t_0)) = \int_0^T w(t_0,T_w)\,|\theta^{mea}(t) - \theta_r'(\mathbf{p}_r(t_0),t) - \lambda_{sw}\theta_h\left(\mathbf{p}_h\left(t_0\right),t\right)|^2\,dt. \quad (12)$$

where T is the measurement duration; w is a non-negative window function, with center position t_0 and width T_w, respectively; λ_{sw} is a switch parameter that takes a value of either 0 or 1 [7]; and $\theta^{mes}(t)$ is the phase measured after the unwrapping. Using the window function w, the unknown parameters are determined at the specified time t_0 with width T_w. For example, t_0 may be changed every second, and T_w is set to a length of approximately one or two periods of the expected waveforms (i.e., respiration and heartbeat). This estimation process is formulated as a minimization problem, which is then solved using the particle swarm optimization (PSO) algorithm [9]. However, when λ_{sw} is 1, it is difficult to estimate all unknown parameters simultaneously due to the imbalance between the contributions from respiration and heartbeat; in particular, in the measured phase data $\theta^{mes}(t)$, the contribution of heartbeats is much smaller than that of respiration. Thus, we use a two-step estimation process [7], as shown in Fig. 1. First, λ_{sw} is set to 0, and only $\mathbf{p}_r(t_0)$ is estimated. Next, $\mathbf{p}_r(t_0)$ is fixed; λ_{sw} is set to 1; and $\mathbf{p}_h(t_0)$ is estimated. This estimation process is repeated from the start to the end of signal using the window function $w(t_0,T_w)$. Finally, the respiration and heartbeat waveforms are reconstructed using Eqs. (10) and (11), respectively, through interpolation over adjacent estimation times (t_{0_1} and t_{0_2}) using the following equation:

$$\theta_*(t) = \frac{t_{0\_2}-t}{t_{0\_2}-t_{0\_1}}\theta_*\left(\mathbf{p}_*\left(t_{0\_1}\right),t\right) + \frac{t-t_{0\_1}}{t_{0\_2}-t_{0\_1}}\theta_*\left(\mathbf{p}_*\left(t_{0\_2}\right),t\right) \quad (13)$$

where $*=r$ denotes the respiration, and $*=h$ denotes the heartbeat. By repeating this calculation, the entire respiration and heartbeat waveforms can be obtained.

4. EXPERIMENTAL RESULTS

In this study, we utilized a MIMO frequency-modulated continuous-wave (FM-CW) radar (Texas Instruments: TI-AW1243) operating in a frequency band ranging from 77 GHz to 80 GHz. The chirp sweep time was 100 µs, and the pulse repetition interval was 30 ms. We used two transmitting antennas and four receiving antennas to construct an eight-element virtual array, and the DC offset and IQ balance were calibrated.

A typical experimental scenario affected by body movement was considered to demonstrate the effectiveness of the modified two-wave model. One healthy participant (a male in his fifties) was observed. The participant remained seated in a chair while measurement was conducted using the MIMO FM-CW radar, which was placed in front of the participant. At the same time, a Piezoelectric Respiration (PZT) sensor and a Blood Volume Pulse (BVP) sensor were attached to his chest and fingertip to measure his respiration and heartbeat, respectively. Fig. 2 shows a photo of the observation process (note: the man shown is not the participant who was observed). Fig. 3 shows the radar image of the participant. A strong echo appearing within the white circle was considered as the target. At maximum power point, the complex signal expressed by Eq. (6) was recorded for 1 min, which was used to estimate the unwrapped phase

FIGURE 2. Measurement setup.

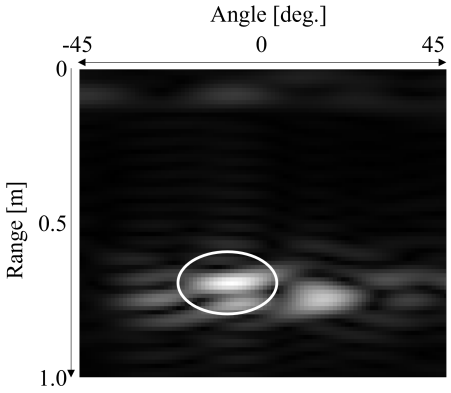

FIGURE 3. MIMO radar image.

$\theta^{mes}(t)$. The data, excluding the first and last 10 s, was used for the analysis. Fig. 4 shows the unwrapped phase; it can be seen that the participant moved slightly (1.3 cm) between 20 and 30 s, causing a phase change of 40 rad. If a person does not lean against the backrest of the chair, this type of movement often occurs in laboratory experiments.

First, we applied the original two-wave model to the measured phase data $\theta^{mes}(t)$. PSO was performed to estimate the unknown parameters in Eqs. (9) and (10) for every second using the two-step estimation process and the cost function shown in Eq. (12). In this case, $\theta_r(\mathbf{p}_\mathrm{r}(t_0), t)$ was used instead of $\theta'_r(\mathbf{p}_\mathrm{r}(t_0), t)$. The maximum order in Eq. (9) was $Q = 2$. The width T_w of the window function w was 5 s for step 1 (respiration). The three waveforms of Eq. (9) using the parameters estimated at 15, 25, and 35 s are shown in Fig. 5. The waveforms evaluated at 15 and 35 s closely match the measured phase waveform $\theta^{mes}(t)$ around the specified times. The waveform evaluated at 25 s is different from the measured phase waveform, and its pattern reflects the body movement observed around the specified time. The respiration waveform reconstructed using Eq. (13), where $* = r$, is shown in Fig. 6. Between 20 and 30 s, no vibrations related to breathing were observed, indicating that the parameter estimation process failed and that Eq. (9) is therefore unsuitable for body movement.

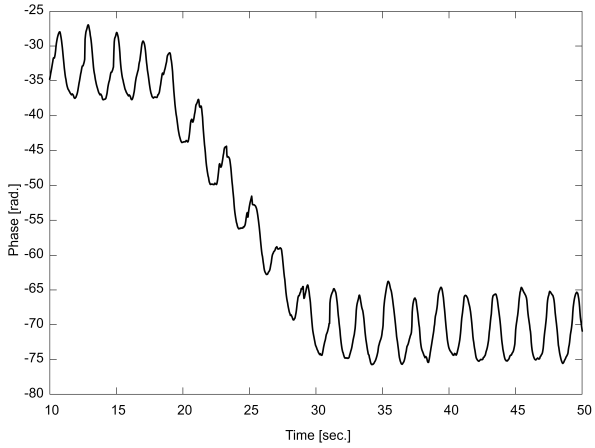

FIGURE 4. Measured unwrapped phase.

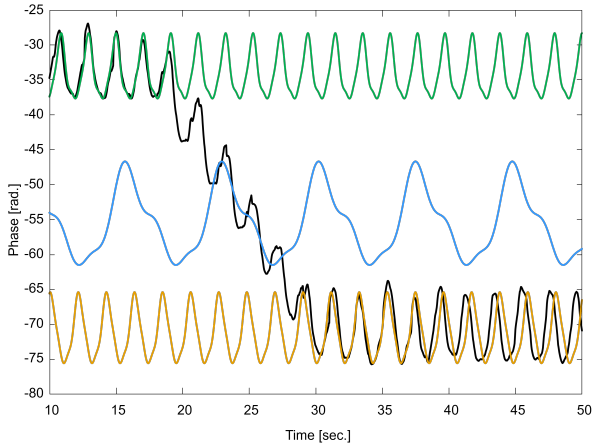

FIGURE 5. Waveforms of Eq. (9) using parameters estimated at 15 s (green), 25 s (blue), and 35 s (yellow), as well as the measured unwrapped phase (black) based on the original two-wave model.

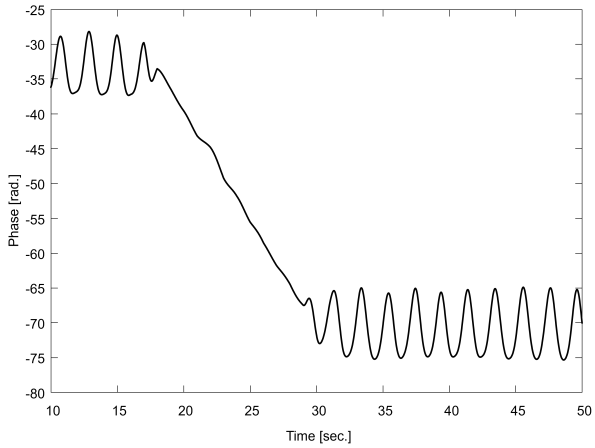

FIGURE 6. Reconstructed respiration waveform based on the original two-wave model.

Next, we used Eq. (11) to estimate respiration in Eq. (12) instead of Eq. (9). The three waveforms of Eq. (11) using the parameters estimated at 15, 25, and 35 s are shown in Fig. 7, which are very similar to the measured phase $\theta^{mes}(t)$ around

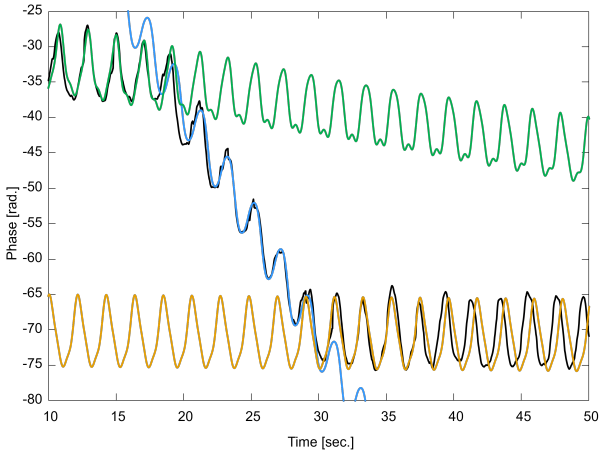

FIGURE 7. Waveforms of Eq. (11) using parameters estimated at 15 s (green), 25 s (blue), and 35 s (yellow), as well as the measured unwrapped phase (black) based on the modified two-wave model.

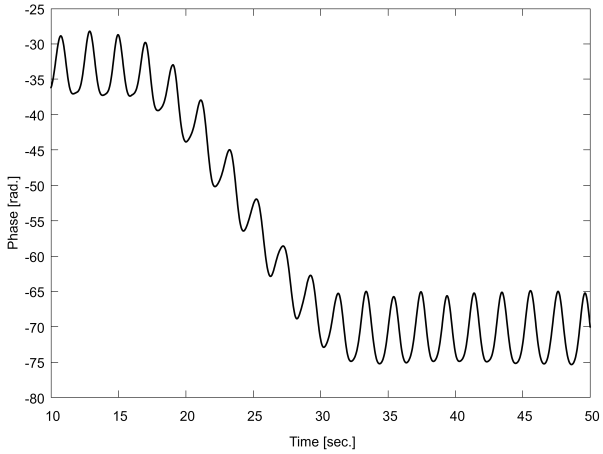

FIGURE 8. Reconstructed respiration waveform based on the modified two-wave model.

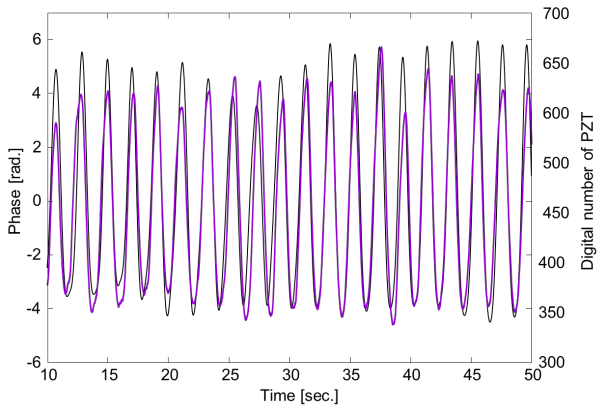

FIGURE 9. Reconstructed respiration waveform with PZT.

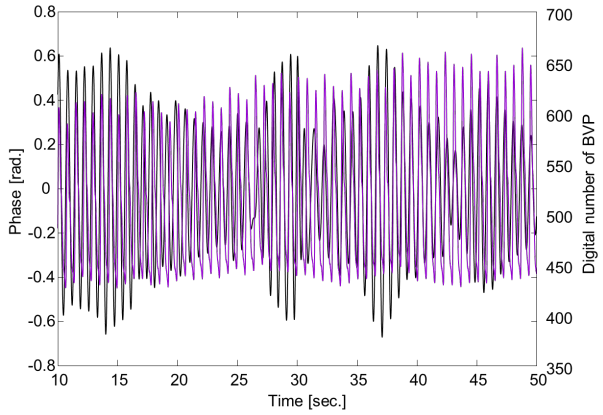

FIGURE 10. Reconstructed heartbeat waveform with BVP.

the specified times. It means that the modified model works both when the target body is stationary (15 and 35 s) and when it is moving (25 s), and the proposed method effectively estimates the time varying property of respiration information. On the other hand, the three waves differ except for the estimated times due to the non-periodic signal. The respiration waveform reconstructed using Eq. (13) with the new parameters is shown in Fig. 8, demonstrating the reappearance of the waveform that disappears in Fig. 6. This waveform can be separated into components related to body movement and respiration. Fig. 9 shows the waveform (black line) of respiration only, with the waveform of the Piezoelectric Respiration (PZT) sensor superimposed in purple. Although the values measured from the two sensors differ, the waveforms are almost identical. Next, the heartbeat waveform was reconstructed using Eq. (13) where $* = h$. In the parameter estimation process using Eqs. (10) and (12), the maximum order was $P = 1$, and the width T_w of the window function w was 2 s for Step 2 (heartbeat). As the BVP sensor was attached to the participant's fingertip, there was a delay in the waveform; in particular, the waveform of the BVP sensor was shifted to the left by 0.36 s. Fig. 10 shows the waveforms of the radar (black line) and Blood Volume Pulse (BVP) sensor (purple line). The peak positions of the two waveforms match well. The results demonstrate that two-step estimation is possible even if the target's body moves slightly. Finally, we calculated the heartbeat's interbeat interval (IBI) using the peak positions of the BVP and radar waveforms. The mean accuracy (*MA*) was calculated using the following equation:

$$MA = 100 \times \left[1 - \frac{1}{M}\sum_{m=0}^{m=M-1} \left|\frac{IBI_{radar}(m) - IBI_{BVP}(m)}{IBI_{BVP}(m)}\right|\right] \quad (14)$$

where $IBI_{radar}(m)$ denotes the m-th IBI sample detected by the radar; $IBI_{BVP}(m)$ is the corresponding sample from the BVP sensor; and M is the total number of heartbeats. Although the *MA* in the static case [7] was 97.09%, it was 93.5% in the present study. For reference, the *ME* (mean error) and *MSE* (mean square error) of IBI in this experiment were 0.00016 and 0.072 s [7]. These results confirmed that the modified method can be used to mitigate the effect of small body movements in laboratory experiments.

Next, we discuss a few issues with the proposed modified method. Although it was able to reconstruct heartbeat and respiration waveforms not only during body movement but also when body movement started and stopped during the observation period, the model still has difficulty in handling high-speed and random body movements. Moreover, although it would be desirable for the maximum order P in Eq. (10) to be 2 or greater considering the asymmetric nature of the heartbeat waveform, P was set to 1 in this study. Furthermore, the accuracy of Eq. (14) decreased from 97.09% to 93.5%. This may be due to the influence of body movement and the asymmetry of the heartbeat waveform. These issues must be considered before the proposed method can be applied in real-world scenarios.

5. CONCLUSION

In this study, we have proposed a modified two-wave model and demonstrate that it can successfully reconstruct respiration and heartbeat waveforms even in measurement scenarios where the original model fails due to target movement. The proposed method was further investigated through a laboratory study. However, the model presents limitations, which we plan to investigate in future research.

ACKNOWLEDGEMENT

We thank K. Komai, who completed a master's course at the Graduate School of Engineering, Nagasaki University, N. Togo at Mitsubishi Electric Engineering and K. Kawajiri and T. Kitamura at Mitsubishi Electric for their help in collecting the experimental data.

REFERENCES

[1] Horimoto, T., T. Konishi, S. Koyama, H. Kawamura, R. Goto, T. Suzuki, M. Hasegawa, S. Hirobayashi, and K. Yoshida, "Heartbeat harmonics detectability during driving simulation using NHA and CW doppler radar," *IEEE Access*, Vol. 11, 51 502–51 514, 2023.

[2] Chian, D.-M., C.-K. Wen, F.-K. Wang, and K.-K. Wong, "Signal separation and tracking algorithm for multi-person vital signs by using Doppler radar," *IEEE Transactions on Biomedical Circuits and Systems*, Vol. 14, No. 6, 1346–1361, Dec. 2020.

[3] Zhang, D., M. Kurata, and T. Inaba, "FMCW radar for small displacement detection of vital signal using projection matrix method," *International Journal of Antennas and Propagation*, Vol. 2013, No. 1, 571986, 2013.

[4] Xiang, M., W. Ren, W. Li, Z. Xue, and X. Jiang, "High-precision vital signs monitoring method using a FMCW millimeter-wave sensor," *Sensors*, Vol. 22, No. 19, 7543, Oct. 2022.

[5] Kakouche, I., H. Abadlia, M. N. E. Korso, A. Mesloub, A. Maali, and M. S. Azzaz, "Joint vital signs and position estimation of multiple persons using SIMO radar," *Electronics*, Vol. 10, No. 22, 2805, Nov. 2021.

[6] Rohman, B. P. A. and M. Nishimoto, "Remote human respiration detection using ultra-wideband impulse radar mounted on a linearly flying platform," *Progress In Electromagnetics Research M*, Vol. 99, 13–22, 2021.

[7] Ko, M. M. and T. Moriyama, "Noncontact monitoring of respiration and heartbeat based on two-wave model using a millimeter-wave MIMO FM-CW radar," *Electronics*, Vol. 13, No. 21, 4308, Nov. 2024.

[8] Ghiglia, D. C. and M. D. Pritt, *Two-Dimensional Phase Unwrapping: Theory, Algorithms, and Software*, Wiley, 1998.

[9] Kennedy, J. and R. Eberhart, "Particle swarm optimization," in *Proceedings of ICNN'95 — International Conference on Neural Networks*, Vol. 4, 1942–1948, Perth, WA, Australia, 1995.

[10] Lv, Q., L. Chen, K. An, J. Wang, H. Li, D. Ye, J. Huangfu, C. Li, and L. Ran, "Doppler vital signs detection in the presence of large-scale random body movements," *IEEE Transactions on Microwave Theory and Techniques*, Vol. 66, No. 9, 4261–4270, Sep. 2018.

[11] Xu, D., W. Yu, Y. Wang, and M. Chen, "Vital signs detection in the presence of non-periodic body movements," *IEEE Transactions on Instrumentation and Measurement*, Vol. 73, 1–16, Aug. 2024.